Numerical investigation of particle spray size distribution in turbulent jet flow

Fathy Saber[a,*], Abouelmagd Abdelsamie[a,b], Momtaz Sedrak[a]

[a]Laboratory of fluid mechanics, mechanical power engineering, Faculty of Engineering (Elmataria), Helwan University, Cairo, Egypt

[b]Laboratory of fluid dynamics and Technical Flows, University of Magdeburg "Otto von Guericke", Magdeburg, Germany.

[*]Corresponding Author: fathi.sabir@m-eng.helwan.edu.eg

Abstract

Injection of spray in turbulent jet flow is involved in many different applications. In this work, a parametric 2D numerical study is performed for a specific configuration similar to a novel burner (SpraySyn) developed at Duisburg-Essent University (Germany). This burner was designed to generate nanoparticle from a spray flame. In order to control the size of nanoparticles, a clear understanding of flow field, temperature and dispersion is necessary. The present study focuses on non-reacting flow (without considering the reaction), to examine the droplet-turbulent interaction. Impact of four different parameters on the flow field, temperature and droplet size distribution, are investigated. These parameters are injection velocity, injection nozzle radius, injected liquid, and injection model. It has been found that increasing the injection liquid velocity from enhances the heat transfer and particle size distribution (due to breakup). The nozzle radius of the injection nozzle has a significant impact on the particle size distribution (PSD) and heat transfer; where increasing the nozzle radius produces small droplets (diameter <67 μm). On the other hand, a decrease in the radius, increases the residence time of the droplet. Using ethanol or n-heptane as injected liquid results in a significant change in the particle size distribution and a minor impact on the flow field. Changing the type of injection model "the single type (monodisperse) and surface type injection (polydisperse)" results in a change in the particle size distribution, at successive time, where more smaller droplets appear in case of the monodisperse compare to the polydisperse.

Keyworks
Spray, Turbulent jet flow, Particle size distribution, Breakup

Nomenclature

d_{lig}	ligament diameter, m
d_{30}	droplet mass mean diameter, m
κ	wave number, 1/m
L_b	liquid sheet breakup length, m
P	pressure of the gaseous flow, N/m^2
P_s	spray pressure, N/m^2
u_j	liquid injection velocity, m/s
u_s	liquid sheet velocity, m/s
W_n	nozzle width, m
W_s	liquid sheet thickness, m
Z	height above the nozzle (vertical distance from the nozzle to the spray measured point), m
r	spray nozzle radius, mm
t	spray time after start of injection, "s" or "ms"

Abbreviations

PIV	particle image velocimetry
PSD	particle size distribution
DPM	discrete phase model
KH	Kelvin Helmholtz

RT	Rayleigh-Taylor
RD	Reitz-Diwakar
TAP	Taylor Analogy Breakup
PE	Pilch–Erdman
VOF	volume of fluid
SMD	sauter Mean Diameter
PaSR	partially stirred reactor
CIJ	continuous inkjet

Greek letters

ΔP_s	spray pressure difference (the difference between the spray pressure of the liquid sheet and the pressure of the surrounding air medium), N/m^2
η	wave disturbance amplitude at distance z from the nozzle, m
η_b	wave disturbance amplitude at breakup point, m
η_o	initial wave disturbance amplitude, m
Λ	wavelength, m
λ_1	wavelength for the liquid sheet breakup, m
ν	kinematics viscosity, m^2/s
ρ_a	surrounding air medium, kg/m^3
ρ_w	water density, kg/m^3
σ	surface tension, N/m
τ_b	liquid sheet breakup time, s

Dimensionless numbers

Re	Reynolds number
We	Weber number

1 Introduction

Spray injection exists in many different applications either in daily life or in industrial applications; for example, perfume, insecticide, spray irrigation, spray coating, painting, combustion, nanoparticle synthesis from spray flame, etc. Even though a lot of research groups around world investigate the spray dispersion, it can be concluded that this dispersion is strongly dependant on the employed configuration. Recently, a group in Duisburg-Essent University (Germany), introduced a novel design for a spray burner aims to generate nanoparticle for spray combustion [1], Various modifications are introduced to this burner, where researchers tried to explore the effect of changing specific parameters, such as the dispersion gas, coflow, mass flow rate, injection liquid velocity. In total, the literature of spray studies can be divided into two main categories: (1) geometry impact (the nozzle shape and pressure, etc), and (2) numerical model's impact. A short review is discussed in the next paragraph.

El-Sayed et al. [2], investigated experimentally the liquid sheet breakup. The liquid was injected from a flat fan jet nozzle caused by pressure-swirling. The effects of nozzle shape and spray pressure on liquid sheet characteristics were investigated for four nozzles with different exit width (1, 1.5, 2 and 2.5 mm). A digital high-speed camera was used to measure the length of the liquid sheet breakup, the velocity of the liquid sheet, and the size of the formed droplets. They compared their experimental results with analytical solutions based on linear and nonlinear hydrodynamics instability theory. They found an excellent agreement between their measurements and the analytical solution with a deviation of 4%-12%; where the breakup length and the droplet sizes formed decreases as the spray pressure difference increases. Schneider et al. [1] introduced the SpraySyn burner design, as a new standard for a free-jet type burner with well-defined and simulation-friendly boundary conditions and geometries, as well as accessibility for optical diagnostics. An oxygen dispersion gas flow is used to aerosolize a combustible precursor solution that is fed through a centrally located capillary. A premixed flat methane/oxygen pilot flame fed through a porous bronze matrix surrounds a stabilizing nitrogen coflow emanating through the same porous matrix, providing easy-to-calculate boundary conditions for simulations. This burner configuration allows the use of a diverse range of solvents, precursors, and precursor combinations. Best-practice operating instructions and parameters are provided, and large-eddy simulations were performed

to demonstrate the burner suitability for numerical simulations. For the same burner, Martins et al. [3] used PIV to measure the gaseous velocity field from the nozzle outlet to positions 26 mm downstream of the SpraySyn burner under a variety of coflow-, pilot-, and dispersion-gas flow rate combinations under non-reacting and reacting conditions with different stoichiometry. This study clarified the importance of the parametric study for this new burner. They found that under reacting conditions, higher mean velocity and standard deviation values are obtained. When chemical reactions occur, the location of the highest velocity fluctuation values shifts downstream. Laser sheet Mie-scattering images and phase doppler anemometry are used by Malte et al. [4] to investigate the atomization characteristics under burning and non-burning conditions for the SpraySyn burner. The effect of the gas-to-liquid volume ratio on spray formation, jet morphology, and turbulence scales in the nozzle far-field is investigated in order to evaluate the performance of the external-mixing gas-assisted SpraySyn-nozzle since the breakup and injection are very important in injection spray. It was observed that raising the feed rate results in reduced droplet and gas velocities. The droplet mean diameter grows along the axial centerline owing to fast evaporation of smaller droplets.

High-speed visualization is used to conduct an experimental investigation of spray formation and flame stability by Bieber et al. [5]. When compared to a standardized burner, an employed variation of nozzle geometry is used to improve spray flame interaction. Spray density and flame fluctuations timescales are quantified and compared, with the latter being significantly larger and thus uncorrelated. Instead, dispersion gas acts as a barrier between the spray phase and the pilot flame; thus, spray ignition is dependent on large liquid lumps with high radial momentum breaking through the dispersion gas. High-speed photos show that the time intervals across peaks of flame activity are substantially longer than the time intervals across peaks of droplet density. As a result, there is no direct relationship between changing droplet density over time and flame activity.

Wang & Zhao [6] investigated the outward-opening piezoelectric injector. Various droplet breakup models were tested in the commercial CFD software STAR-CD and validated with measurements. The injection pressure was kept constant at 180 bar, and two different back pressures 1 and 10 bar were used to test the robustness of the breakup models. To clarify the overall performance of different breakup models in modelling gasoline sprays, the effects of mesh quality, simulation timestep, and breakup model parameters were investigated. It is discovered that the tuned Reitz-Diwakar (RD) model performs well under a variety of back pressures, and the spray penetration agrees well with experimental measurements. The modified Kelvin-Helmholtz-Rayleigh-Taylor model (KH-RT), on the other hand, was unable to achieve good agreements with fixed model parameters at different back pressures. At 10 bar backpressures, the tuned KH-RT model shows a much faster breakup process, resulting in abnormal spray patterns and fuel vapors distributions.

In order to describe the fuel atomization and breakup process, different spray models and different spray nozzles have been developed for CFD simulations and some are compared with experimental results. To calculate complex interactions between sprays and gas motions, the Reitz-Diwakar (RD) breakup model was presented by Reitz and Diwakar [7]. Reitz [8] presented the wave model by exploiting Kelvin-Helmholtz (KH) instabilities in liquid jets. The Rayleigh-Taylor breakup model, proposed by Taylor [9], considers the unstable RT waves due to the rapid deceleration of the drops. The KH-RT hybrid breakup model, consisting of both the KH and RT instability theories, was then proposed by Reitz and Beale [10] to predict both diesel and gasoline sprays. The Taylor Analogy Breakup (TAB) model was used to calculate droplet breakup for engine sprays by Amsden and Anthony [11]**.**

The impact of boundary conditions on the breakup was investigated by Ann and Fergusson [12]. They used ANSYS-Fluent to evaluate different breakup model by comparing their results with the doppler particle analyzer measurement “PDPA”, secondary breakup model theory, and collision model theory. The influence of nozzle shape on microfluidic inkjet breakup is investigated by Rosello et al. [13].

First, an industrial ink used in continuous inkjet (CIJ) printing devices is selected. Fluid is jetted at high speed (10m/s < U < 20m/s) through an axisymmetric micro–nozzle ($D_{out} \cong 50\mu m$). Four different nozzle designs with the same exit radius were tested, the visualization software JetXpert imaging system is used to display a static image. The examination of droplet behavior and macroscopic atomization characteristics of a non-reacting liquid spray via a series of large-eddy simulations is investigated by Sula et al. [14]. In this study, they compared the predictions of three popular spray atomization models, namely TAB, RD, and Pilch–Erdman (PE) models, with an available experimental data. According to their simulations, the TAB model outperforms the other two models slightly, as a conclusion the TAB model produces slightly more accurate predictions for the liquid penetration. This is because it better encapsulates the underlying physical mechanisms of droplet breakup.

All three pre-existing models, on the other hand, overestimate fuel vapor penetration. The numerical tests also show that the proposed TAB model has the potential to improve accuracy in calculating liquid and vapor

penetration distances. However, when compared to experimental data, the vapor penetration distance is still slightly overestimated. Assessment and validation of liquid breakup models for high-pressure dense diesel sprays is investigated by Ren and Li [15]. In this paper, the numerical simulation was implemented using the Converge CFD code. It is found that the modified KH-RT breakup model gives the most reasonable predicted results in both engine simulation and high-pressure diesel spray simulation. For the standard KH-RT model, the model constant has very significant impact on the result which is required carful calibration. The TAB model and the RT model do not provide reasonable predictions for high-pressure spray characteristics as well as simulated engine performance and emissions.

Using Gambit and FLUENT software, Sapee [16] investigated a droplet size such as Sauter Mean Diameter (SMD) for kerosene fuel using 2D Discrete Phase Model (DPM) with 2D axisymmetric and particle diameter for kerosene fuel using 3D Discrete Phase Model with 30° swirl. They found that, the k-epsilon model is able to correctly predict the droplet size and spray behavior of kerosene fuel. Where increasing the pressure difference resulted in a decrease in the droplet diameter and an increase in droplet velocity. The spray process of the injected liquid was analyzed by Weise et al [17] using volume of fluid (VOF) calculations and validated by shadowgraph imaging which provided the size distribution and the mean velocity of the droplets. A side illuminated long exposure image of the spray was used to calculate the spray angle. The spray properties that resulted (droplet sizes, velocity, and spray angle) were used as injector boundary conditions in downstream combustion simulations. The spray and gas phases of the flame were simulated using Euler–Lagrange method, turbulence was modelled using the RNG k-epsilon model, and turbulent combustion was described as a partially stirred reactor (PaSR). They concluded that, the VOF simulation and experiment agreed qualitatively and quantitatively.

From all of these publications, it can be concluded that for the SpraySyn burner configuration, there is no publication focused on the spray dispersion and spray dynamics. Furthermore, to the authors knowledge, the impact of injection speed, nozzle diameter, fuel type, injection models on the spray dispersion were studied in the SpraySyn configuration. The present study concentrates on the SpraySyn burner configuration for non-reacting flow. The spray configurations and its dispersion will be numerically investigated. Also, several parameters such as injection flow speed, injection model, nozzle diameter and injected liquid type will be studied with testing their impact on the flow field and the particle size distribution. Different numerical models will be examined/evaluated with using discrete phase model implemented in ANSYS-FLUENT. Consequently, the present study will consider the effect of injection velocity, injection nozzle radius, injected liquid type, and injection model on the performance of SpraySyn burner for non-reacting flow. The spray configuration and its dispersion are numerically investigated for two-dimensional flow using ANSYS-Fluent, the used software is validated using published experimental results [2].

This paper is organized as follows, the first section discusses the numerical models, second section review the validations of employed models, third section discusses the investigated geometry and configuration, The results are discussed in details in section four. At the end, the conclusion closes the paper in section five.

2 Numerical Models for Spray Dynamics

All simulations are performed using ANSYS-FLUENT 19.1. Four essential models are activated to conduct this study (1) Discrete Phase Model "DPM", (2) Injection model, (3) Turbulent model "$k-\varepsilon$", and (4) Breakup model "KH-RT".

To ensure that the employed model is working in a proper way, a validation is needed. For this purpose, a case from El-Sayed et al. [2], has been compared, as it will be seen in the next section. The simulation performed for five values of pressure difference, ΔP_s= 120 kPa, 150 kPa, 200 kPa, 250 kPa and 280 kPa. To evaluate the validity of the employed models, two main parameters are used for comparison between the experimental and numerical data. The first parameter is Breakup length L_b & the second parameter is Relative particles mean diameter $d_{30}/d_{30,ref}$, where $d_{30,ref}$ is a reference case at ΔP_s= 120 kPa.

3 Validations of the Employed Models

As it discussed, the validation will be performed by comparing the current simulation with the experimental

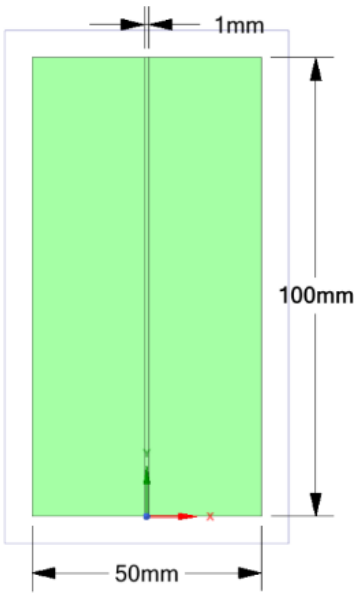

Figure 1 Domain used for the study of flat fan nozzle of W_n = 1 mm.

In this comparison, the jet speed calculated as in [2],

$$u_s = \left(\frac{2\Delta P_s}{\rho_w}\right)^{\frac{1}{2}} \quad (1)$$

A qualitative comparison has been done by comparing the images of the spray obtained from [2] with the velocity contours obtained from the present simulation as shown in Figure 2. This figure depicts the comparison at different injection pressure ΔP_s of 120 kPa, 150 kPa, 200 kPa, 250 kPa, and 280 kPa. As it can be observed, both experiment and simulation show broader jet with increasing the injection pressure. Even though this comparison shows that the simulation predicts roughly the shape of the jet, an accurate comparison can't be obtained from this figure. Therefore, the breakup length and the relative droplet mean diameter versus the pressure difference (ΔP_s) will be compared in Figure 3 and Figure 4, respectively. For validation of the breakup length L_b, there is a simple method suggested here to determine L_b from the Lagrangian approach "DPM". In this method, the breakup starts when the width of the particle parcel reaches a specific value (breakup threshold). Three thresholds are tested and compared with the breakup obtained from the experiment: 1.8, 1.9, and 2 times the initial width. It was found that the breakup threshold number 3 shows the best agreement and it is used in Figure 3. In Figure 3 and Figure 4, three data appear, (a) theoretical values [2] , (b) experimental values [2], and (c) present simulation. From these figures, it can be seen that, the comparison shows good agreement between the present simulation and the experimental data. Where, the water sheet breakup length and the droplet mass mean diameter ratio decrease with increasing the spray pressure difference ΔP_s in the same trend as that in the reference data. This section demonstrates that, the employed models for spray dispersion can be used for further simulation as it will be done in the next section.

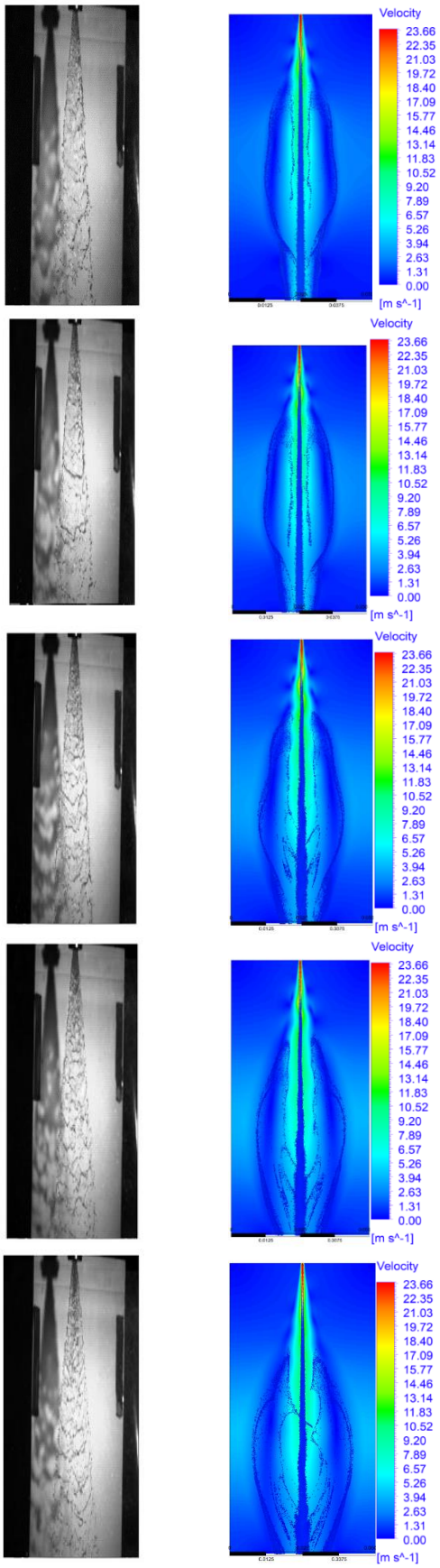

Figure 2 Comparison between the experimental work [2] and the present numerical simulation for different injection pressure; from top to bottom 120 kPa, 150 kPa, 200 kPa, 250 kPa, 280 kPa. Left: Spray image obtain by experiment. Right: Contour of the velocity magnitude of the present simulation.

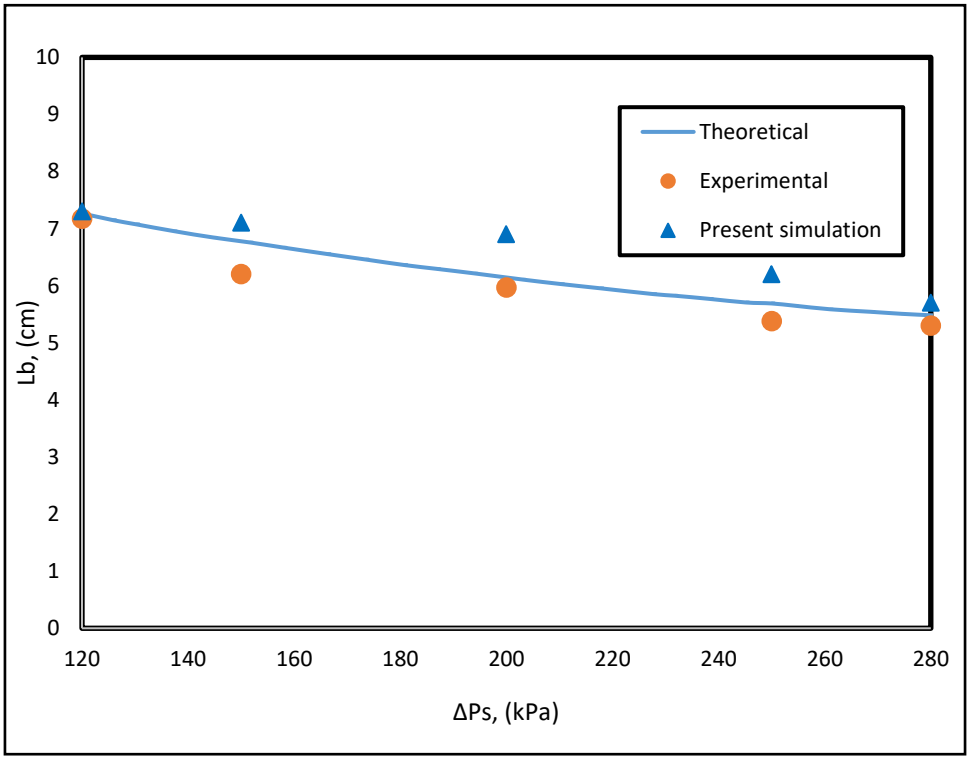

Figure 3 Effect of spray pressure difference on the breakup length. Comparison between the theoretical, experimental data [2], and the present simulation.

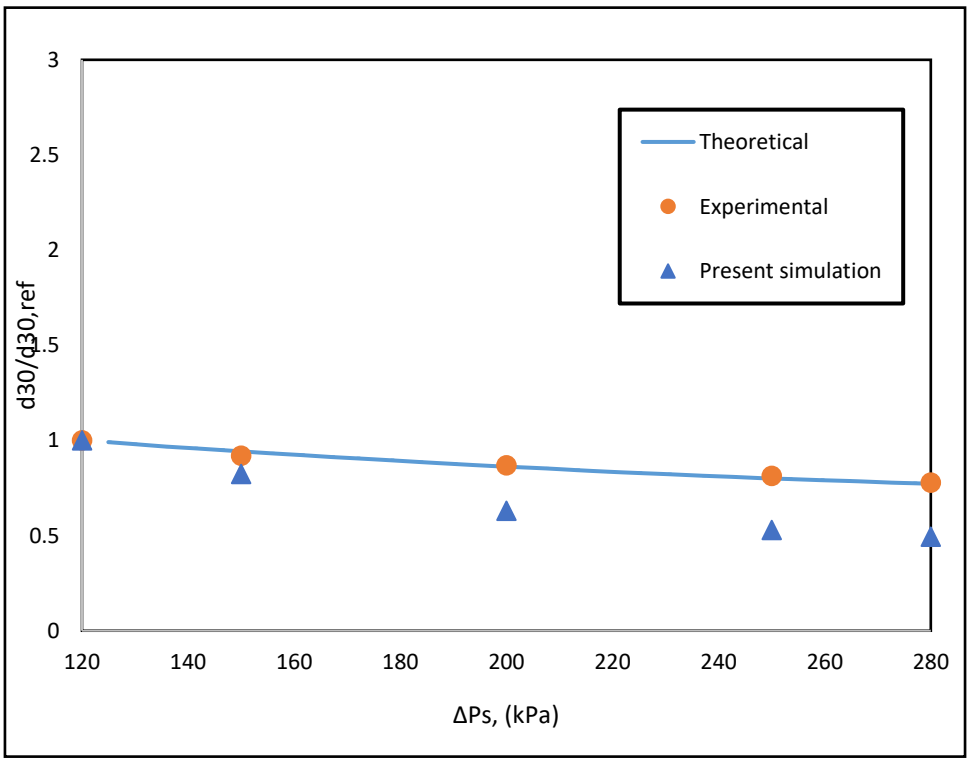

Figure 4 Effect of spray pressure difference on the droplet mass mean diameter ratio. Comparison between the theoretical, experimental data [2], and the present simulation.

4 Investigated Geometry and Configuration

The main objective of the current study, is to simulate configuration and geometry similar to that developed at Duisburg University [1], which is called a SpraySyn burner. In this section, the computational domain and experimental configuration which are used for the study of SpraySyn burner nozzle are reviewed, then the current employed numerical model are discussed.

4.1 Existing Experimental Configuration

The SprySyn burner configuration is schematically illustrated in Figure 5, which contains a circular burner with three main outlets with dimensions are summarized in Table 1 [1].

1. Center outlet used for dispersion flow which is a mixture of liquid (ethanol or n-heptane) and air at temperature 300 K
2. Second annulus opening for pilot flame at temperature of 2500 K.
3. Third outlet is for coflow at temperature of 300 K

In the current simulation, the pilot flame and the coflow will be replaced with hot air at temperature of 2500 K and cold air at temperature of 300 K, respectively.

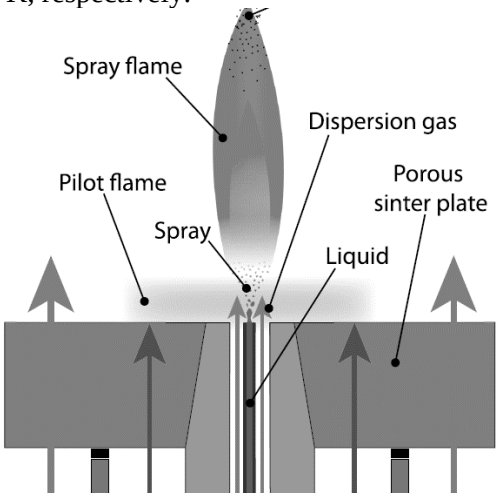

Figure 5 Schematics diagram of the SpraySyn burner **[1]**.

4.2 Initial Conditions for The Current Simulation

The ultimate purpose of this work is to study the effect of (1) injection liquid speed ($u_j = 30, 60$ and 91.34 m/s), (2) radius of the injection nozzle ($r = 0.75, 1.5$ and 2.25 mm), (3) injected liquid type (ethanol and *n*-heptane) and (4) injection model type (monodisperse and polydisperse), on the breakup of the liquid spray. The initial conditions are summarized in Table 1

Table 1 Initial Conditions

	Dispersed flow	**Pilot flow**	**Coflow**
Fluid type	Air and liquid ethanol/n-heptane	Air	Air
Temperature	300 K	2500 K	300 K
Injection liquid speed(m/s)	30, 60 & 91.34	3.71	0.637
Inner radius (mm)	0	4	15
Outer radius (mm)	0.75, 1.5 & 2.25	15	35

4.3 Numerical Models Used in The Present Work

As discussed before, all simulations are performed using ANSYS-FLUENT 19.1. Four essential models are activated to conduct this work (1) discrete phase model "DPM", (2) injection model, (3) turbulent model "SST 4 equations", (4) breakup model "KHRT". All simulation was running for a physical time of 6.3 ms.

4.4 Numerical Domain and Geometry

Figure 6, shows the computational domain. The geometry and the computational domain are generated using the Space Claim. The 2D dimension is 150 mm x 150 mm. Initially, the domain is filled with air at temperature of 300 K.

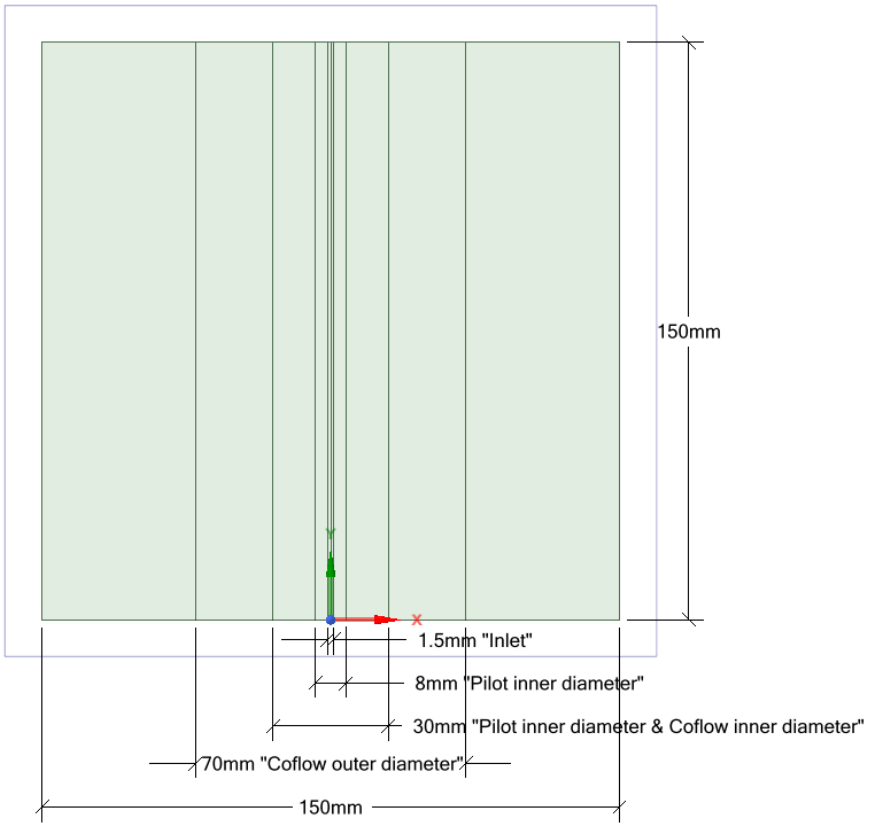

Figure 6 Computational 2D domain model shows inlets of the dispersion mixture, pilot flow, and coflow.

5 Results and Discussion

Impact of four different parameters will be examined and discussed in this section: (1) injection velocity, (2) injection nozzle radius, (3) injected liquid type, and (4) injection model.

5.1 Effect of Injection Velocity

The impact of changing the liquid "ethanol" injection velocity is investigated in this section, where three velocities are tested: u_j=30 m/s, 60 m/s & 91.34 m/s at $r = 0.75$ using monodisperse as an injection model. There are typical injection speeds found in different spray injection applications. Figure 7 shows the contour of the gas velocity magnitude for the three tested velocities at different simulation instances. As it is expected, in the case with higher injection speed ($u_j = 91.34\ m/s$), the gas reaches the outlet boundary first. Also, broader profile of the gas velocity is observed. Follow the photos from left to right for the same time as a result of increasing injection velocity (u_j).

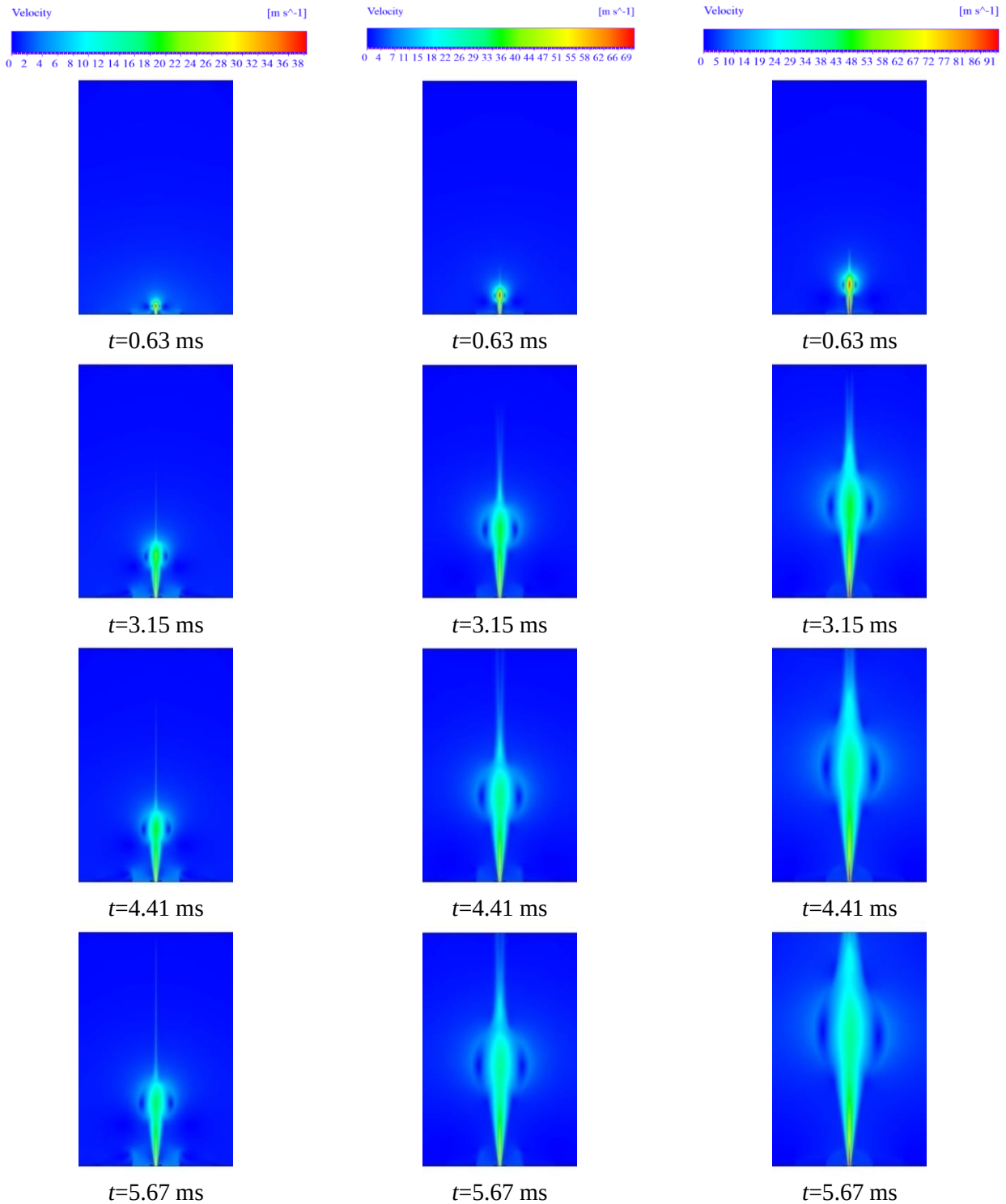

Figure 7 Contour of the gas velocity at different time instances for different injection velocity. Left: uj =30 m/s. Centre: uj=60 m/s. Right: uj =91.34 m/s.

The behaviour of the gas velocity reflects directly on the temperature distribution. Faster spray, u_j =91.34 m/s, pull the hot air (jet entrainment) to the core region as it can be observed from Figure 8. Where this figure shows the contour of the temperature in the background and the dispersed droplet (colored spheres in the middle of the domain). The dispersed droplet is colored by the liquid temperature; the size of these droplets in this figure is scaled up for visualization. It is worth mentioning that the spray in the case with faster spray injection, u_j =91.34, shows higher liquid temperature (Figure 8 Right). This is due to the speed of the carrier gas, where high speed results in faster heat transfer from the gas to the liquid. Furthermore, Figure 8 shows that, near to the nozzle,

the pilot flow temperature profile is similar and nearest to the experimental and real cases, especially at later time *t*=5.67 ms.

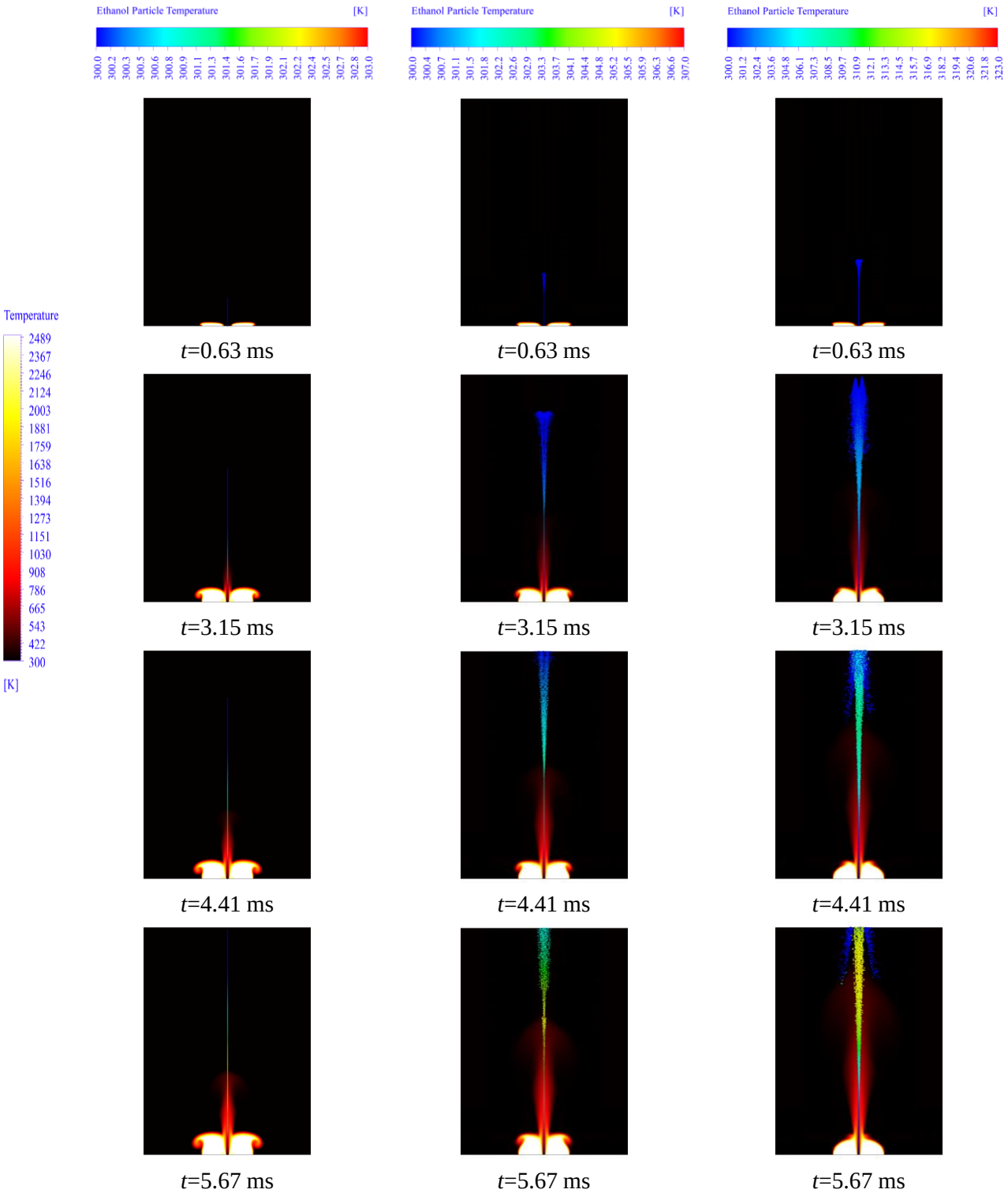

Figure 8 Development of flow and particle temperature of three dispersed flow velocities with time after start of injection Left: u_j =30 m/s. Center: u_j=60 m/s. Right: u_j=91.34 m/s.

The behaviour of the velocity and temperature have a direct impact on the particle size distribution (PSD) as it is depicted in Figure 9. At the beginning of the simulation, *t*=0, all three cases have the same PSD. with time, these distribution starts to deviate and strongly changes as it can be observed from Figure 9. This is due to the

breakup which increases with the increase in the injection velocity. Case with higher injection velocity creates smaller particles sizes, in range from $32\ \mu m\ to\ 126\ \mu m$, as it can be observed from Figure 9 (Right) at t=5.67 ms. Additionally, the range of small particle sizes decrease with the decreasing of the injection velocity as shown in Figure 9 and Table **2**, where for the lowest injection velocity the breakup is relatively weak because the injection velocity is not sufficient and the Weber number is smaller than the case with u_j=91.34 m/s.

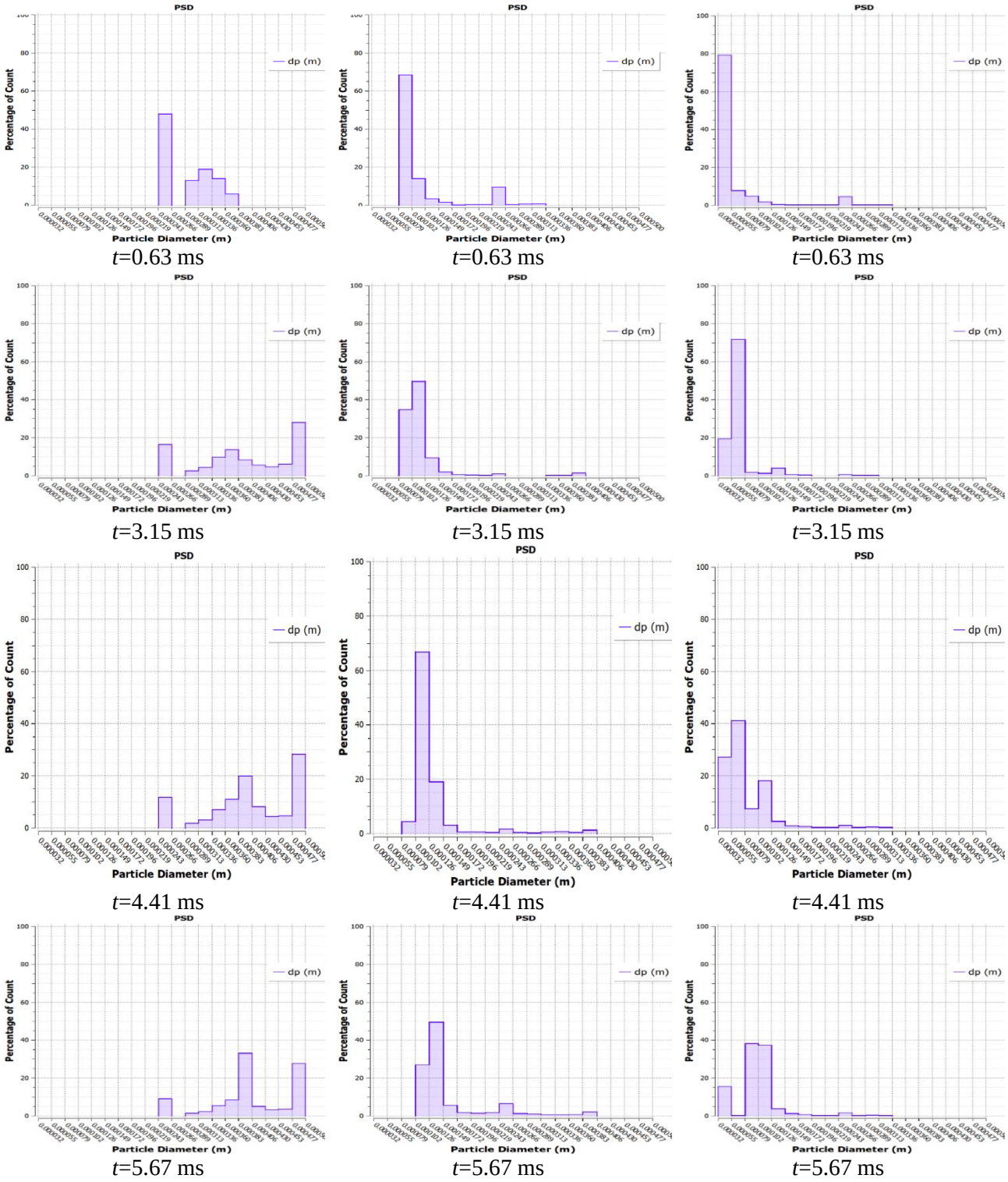

Figure 9 PSD for different injection speed, with different time instances. Left: u_j=30 m/s. Centre: u_j=60 m/s. Right: u_j=91.34 m/s.

Table 2 Ranges of particle diameters for different injection speed at different time instances.

Particle size range [μm]	Time after start of injection	$u_j = 30\ m/s$	$u_j = 60\ m/s$	$u_j = 91.34\ m/s$
32-126	*t*=0.63 ms	0%	85%	90%
	t=3.15 ms	0%	85%	95%
	t=4.41 ms	0%	70%	95%
	t=5.67 ms	0%	38%	90%
126-219	*t*=0.63 ms	0%	7%	5%
	t=3.15 ms	0%	5%	3%
	t=4.41 ms	0%	22%	3%
	t=5.67 ms	0%	52%	8%
219-313	*t*=0.63 ms	68%	8%	3%
	t=3.15 ms	25%	7%	2%
	t=4.41 ms	20%	5%	0%
	t=5.67 ms	10%	3%	2%
313-406	*t*=0.63 ms	32%	0%	2%
	t=3.15 ms	25%	3%	0%
	t=4.41 ms	13%	3%	2%
	t=5.67 ms	20%	3%	0%
406-500	*t*=0.63 ms	0%	0%	0%
	t=3.15 ms	50%	0%	0%
	t=4.41 ms	67%	4%	0%
	t=5.67 ms	70%	4%	0%

5.2 Effect of Injection Nozzle Radius

The impact of varying the injection nozzle radius "r" is examined in this section, where three radii, r = 0.75 mm, 1.5 mm, and 2.25 mm are used at $u_j = 91.34\ m/s$ using monodisperse as an injection model and ethanol as a liquid. Figure 10 depicts the contour of the magnitude of the gas velocity for the three tested radii at various simulation times.

As observed, in the case of increasing the nozzle radius with keeping the parameters of the pilot flow (velocity, inner radius and outer radius), the injection gas Reynolds number ($\mathrm{Re} = 2\ u_j\ r/\nu$) and the volume flow rate of the carrier gas are increase. Wider jet is observed with increasing the jet nozzle diameter as it can be observed from Figure 10. Flow with larger volume flow rate, higher Reynolds number, larger nozzle diameter can expand wider and penetrate the surrounding flow faster. This explains why the gas reaches the outlet first in the case of r = 2.25 mm in Figure 10(Right).

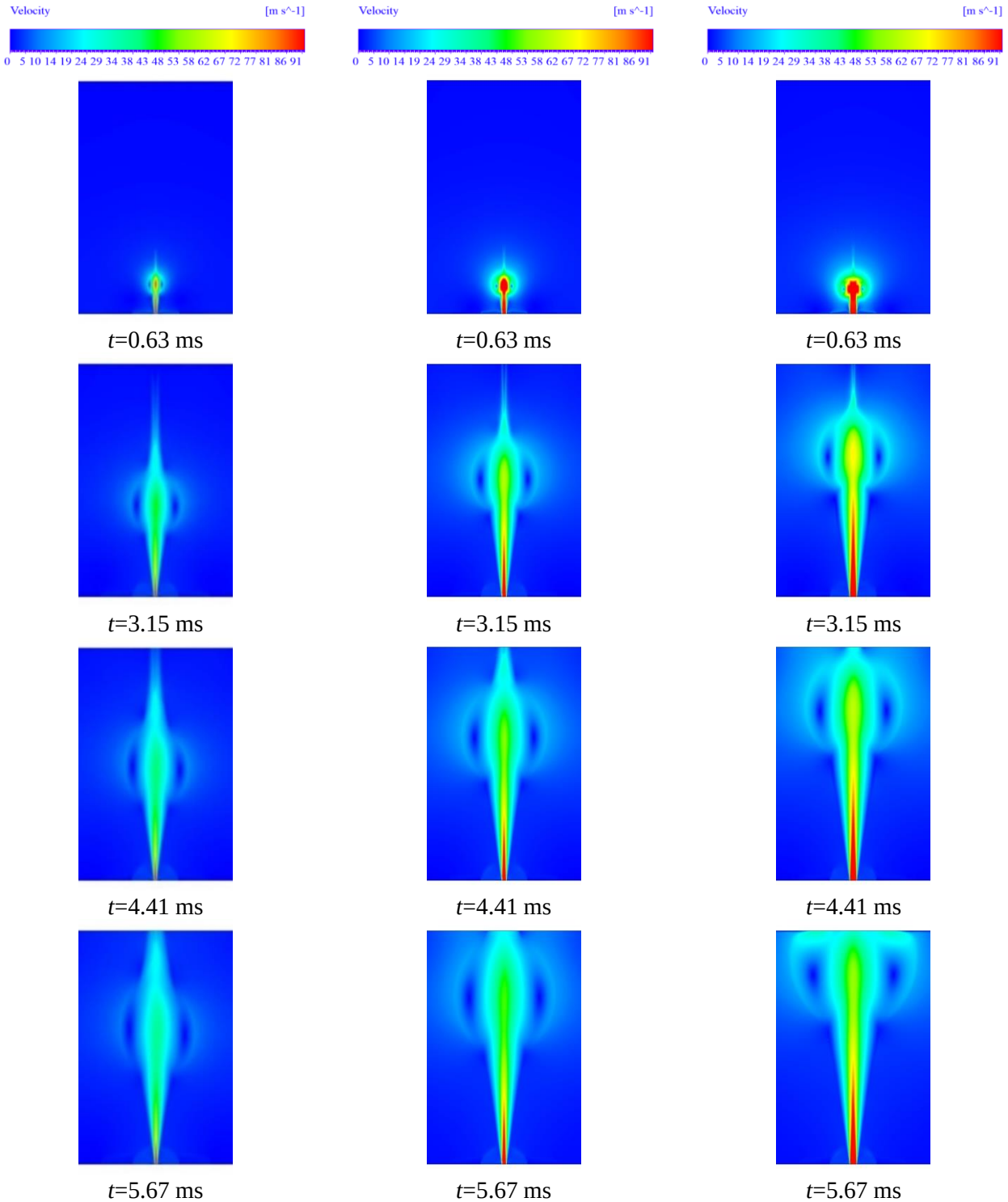

Figure 10 Velocity contours of different nozzle radius at different times instances. Left: r=0.75 mm. Center: r=1.5 mm. Right: r=2.25 mm.

Increasing the nozzle radius, means increasing the width of the jet core region with low temperature (T=*300* K), on the other hand the case with smaller radius *r=0.75* mm, has the hot air very close to the core of the jet as it seen from Figure 11(Left). This enhances the heat transfer in the case of *r=0.75* mm, therefore the droplet become hotter as in Figure 11 (Left). The spray in the case with smaller radius (lower Reynolds number), has longer residence time. As a consequence, the droplets have enough time to transfer the heat with the surrounding hot gas, and breakup into smaller droplets due to the heat transfer and the velocity differences.

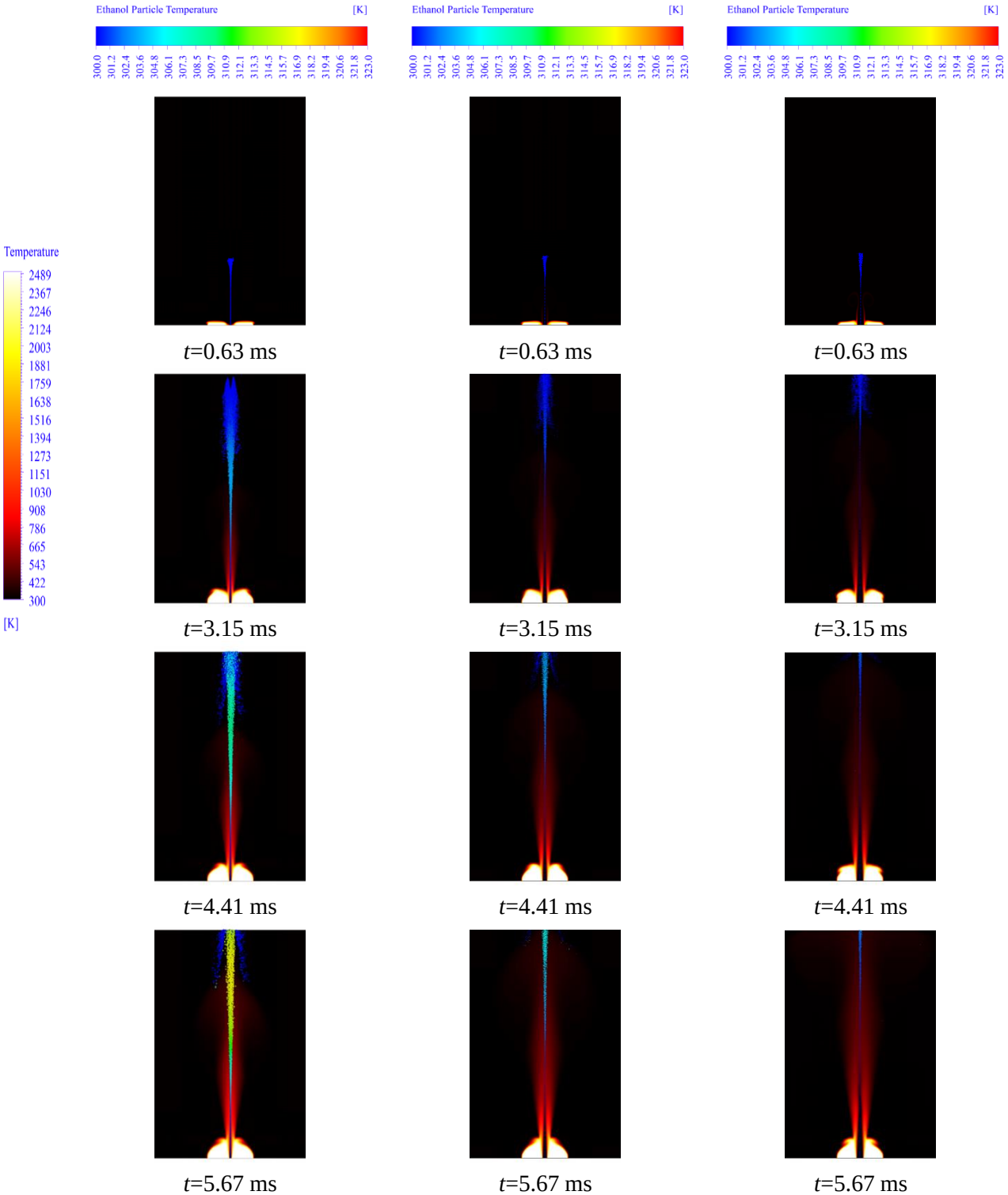

Figure 11 Development of flow and particle temperature of three dispersed flow nozzle radius with time after start of injection. Left: r=0.75 mm. Center: r=1.5 mm. Right: r=2.25 mm.

This explanation is supported by (Figure 12 Left), where more droplet can be found with small diameter range $32\ \mu m\ to\ 119\ \mu m$. In the cases with shorter residence time (case with *r=2.25* mm), or faster jet penetration, the droplets leave the domain very fast, therefore, they don't have enough time to exchange the heat or break to smaller diameter, as a consequence particle with larger size can be observed as in Figure 12 Right with diameter range $[> 54\ \mu m]$. The case with r=1.5 mm (Figure 12 Centre), shows actually both large and small droplets size compared to the case with r= 2.25 mm which shows mostly unified size (Figure 12 Right), and compare with the case with r=0.75 mm (Figure 12 Left).

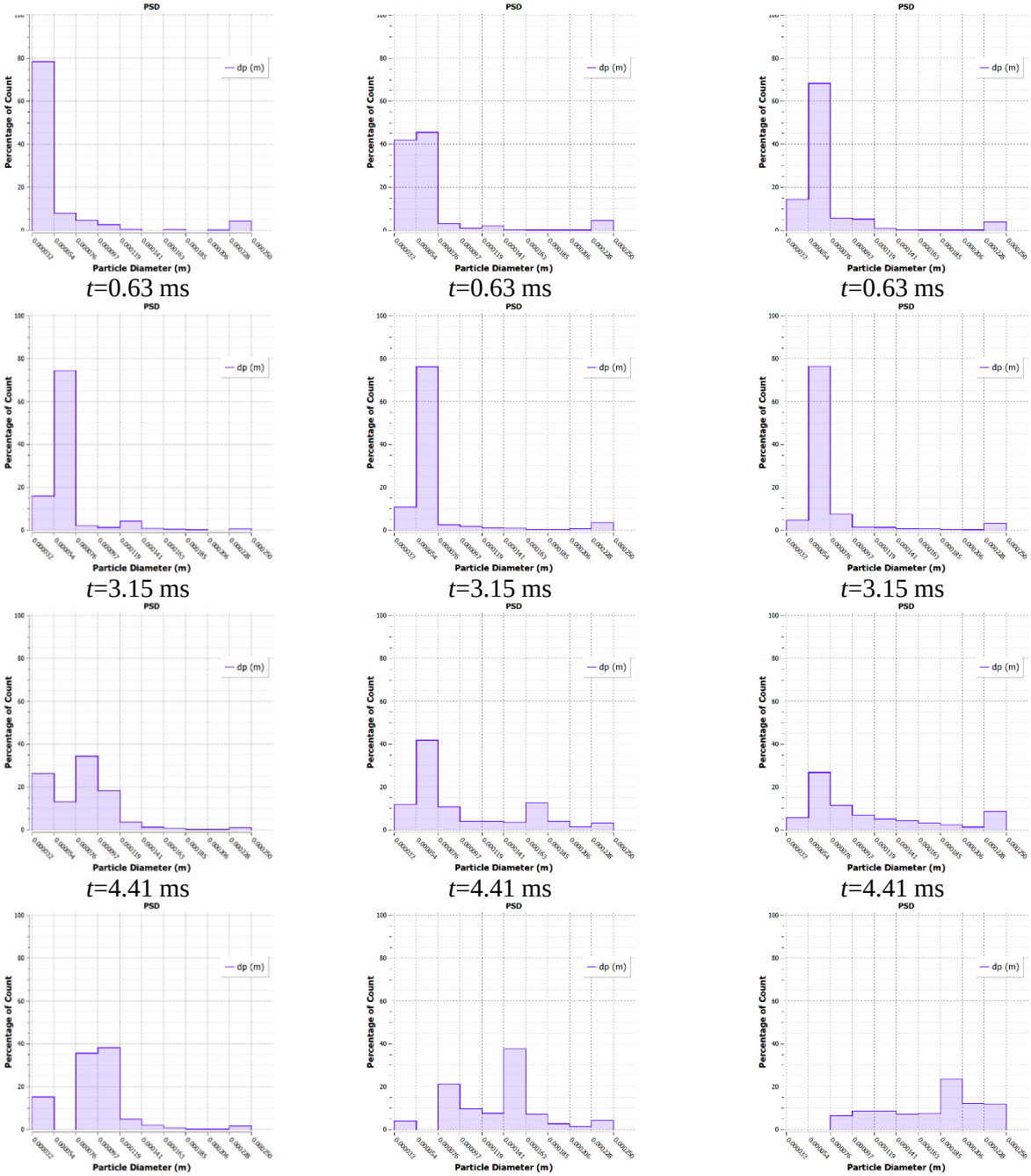

t=0.63 ms *t*=0.63 ms *t*=0.63 ms

t=3.15 ms *t*=3.15 ms *t*=3.15 ms

t=4.41 ms *t*=4.41 ms *t*=4.41 ms

t=5.67 ms *t*=5.67 ms *t*=5.67 ms

Figure 12 PSD of different dispersed flow nozzle radius at different times after start of injection. Left: r=0.75 mm. Centre: r=1.5 mm. Right: r=2.25 mm.

5.3 Effect of Injected Liquid Type

The effect of varying the injected liquid is examined and discussed in this section at $u_j = 91.34\ m/s$ and $r = 0.75\ mm$ using monodisperse as an injection model and ethanol as a liquid, two different injected liquid (ethanol and n-heptane) are examined. They are common in spray combustion applications. Therefore, the goal of the current work is to examine the effect of changing the liquid (physical and thermodynamics properties) on the flow field and the particle size distribution in the SpraySyn configuration. Figure 13 depicts the contour of the gas velocity for both liquids at various simulation times. As shown in Table 3, the density, the dynamic viscosity, the thermal conductivity and the specific heat of the heptane are smaller than of the ethanol. These are liquid

properties, since there is no evaporation considered, the gaseous flow fields for both cases should be same, as it can be seen from Figure 13.

Table 3 Physical Comparison Between Ethanol and n-Heptane.

	Ethanol	n-Heptane
Density (kg/m^3)	790	684
Thermal Conductivity ($W/m.K$)	0.182	0.14
Specific heat at constant pressure ($J/kg.K$)	2470	2219
Dynamic Viscosity ($kg/m.s$)	0.0012	0.000409
Kinematic Viscosity (m^2/s)	0.00000152	0.0000006
Vaporization Temperature (K)	271	271
Droplet Surface Tension (N/m)	0.022348	0.0198263

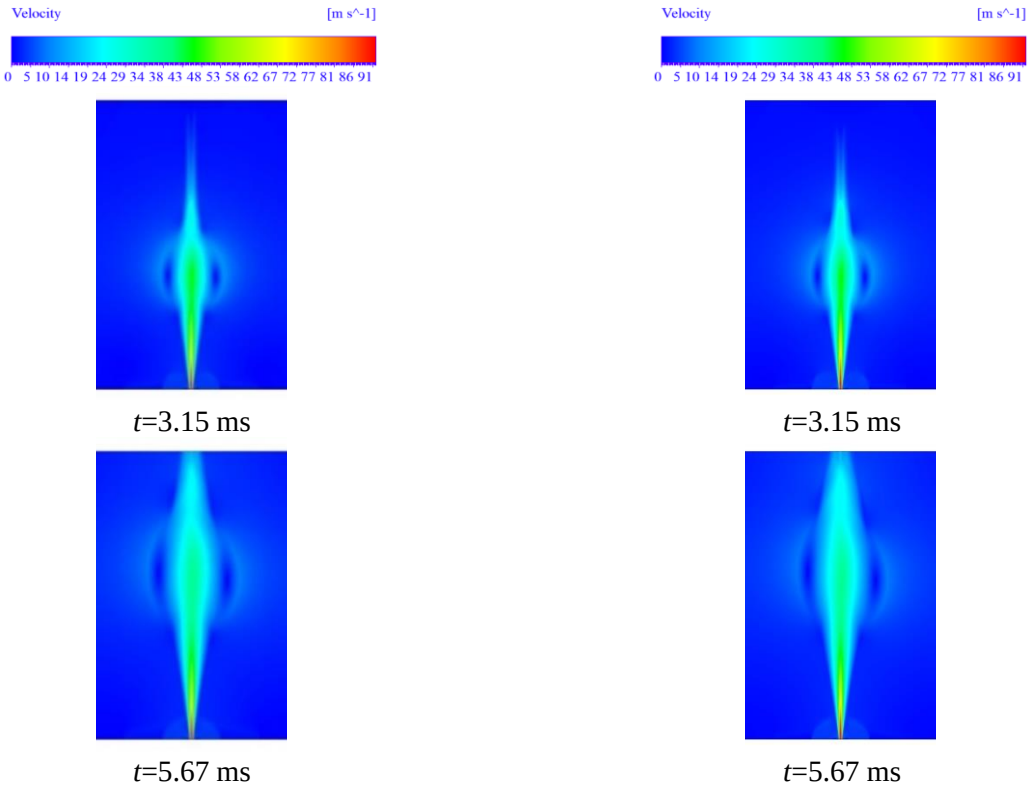

t=3.15 ms *t*=3.15 ms

t=5.67 ms *t*=5.67 ms

Figure 13 Velocity contours of different dispersed fluid type at different times after start of injection. Left: Ethanol. Right: n-Heptane.

In contrast with the impact of the liquid droplet on the gaseous velocity field, it has been found that the thermal and thermodynamics properties have a significant impact on the temperature field as it can be seen from Figure 14. Where higher temperature colored the droplets in case of ethanol. This due to that the thermal conductivity and the specific heat of the ethanol are larger than those of n-heptane (Table 3).

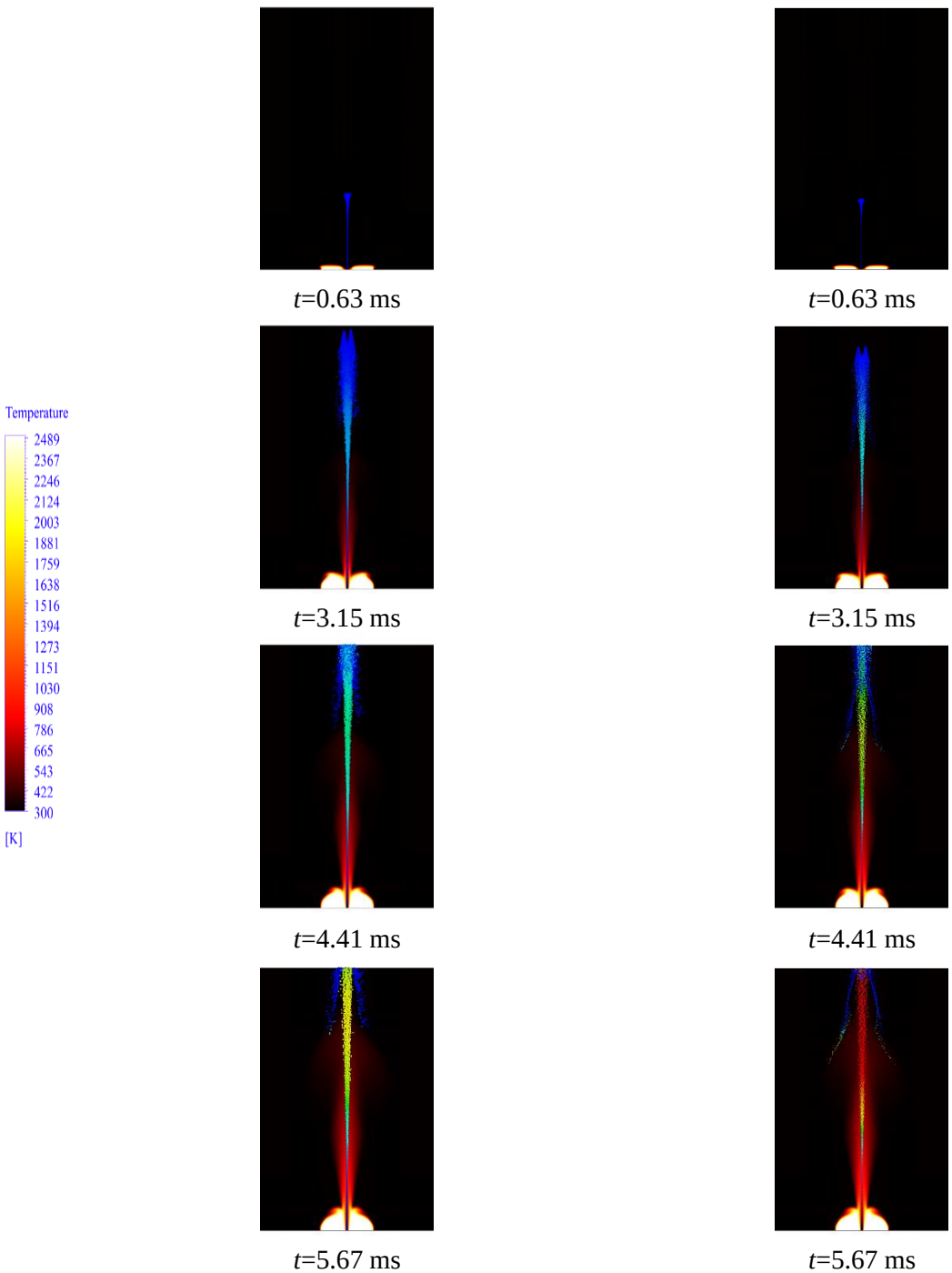

Figure 14 Development of flow and particle temperature of two dispersed fluid with time after start of injection. Left: Ethanol. Right: n-Heptane.

No huge changes in the particle size distribution are observed, only at the later time (*t*=5.67 ms), where the droplets of ethanol have higher temperature (Figure 15). At this instance, the breakup becomes more pronounced, therefore, variant size of droplet can be observed compare to that of n-heptane droplets.

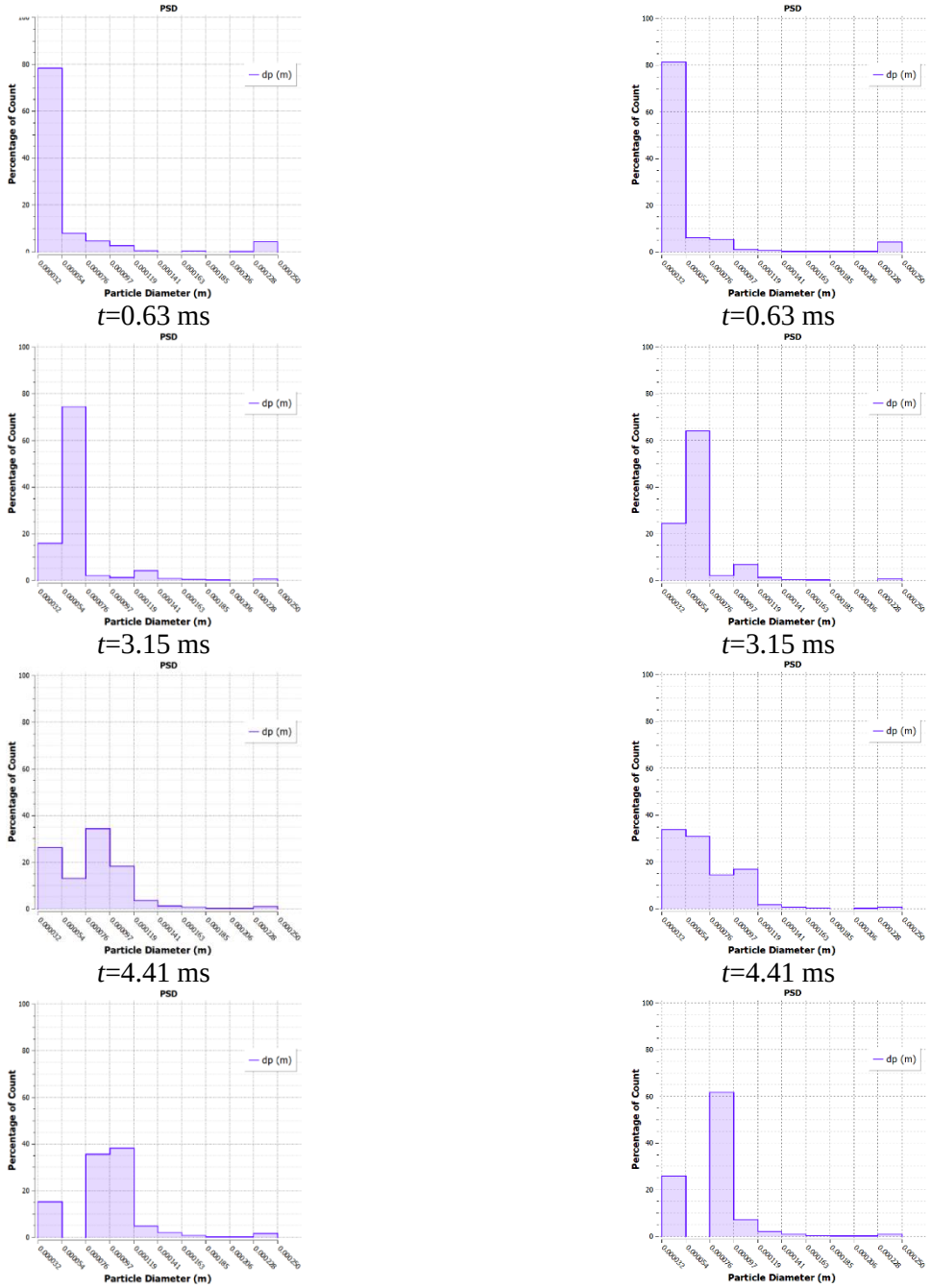

t=0.63 ms *t*=0.63 ms

t=3.15 ms *t*=3.15 ms

t=4.41 ms *t*=4.41 ms

t=5.67 ms *t*=5.67 ms

Figure 15 PSD of different dispersed fluid type at different times after start of injection. Left: Ethanol. Right: n-Heptane**.**

5.4 Effect of Injection Model

In this section, two important numerical initializations are applied for ethanol at $u_j = 91.34\, m/s, r = 0.75\, mm$. They are common use in the ANSYS-FLUENT: (1) single type injection (monodisperse), (2) Surface type injection (polydisperse). Where many researchers are using these two models without quantifying their impact. Of course, it doesn't make any sense to explain the physical difference between them, since they both are supposed to apply the same physics. The direct comparison is to check the PSD as in Figure 16. The simulation with these models produces different PSD. At an early stage, both distribution gives the same result (*t*=0.63 ms), as expected; with time they deviate from each other. Where smaller droplets appear in case of the surface type injection (polydisperse) compare to the single injection one (monodisperse) which show more

larger particles. This leads to very important conclusion; more experiments and tests are needs to be validate which model is more promising in numerical analysis. Though the beginning is approximately the same (t=0.63 ms), the development of PSD is different with time. This will be considered in our near future publications.

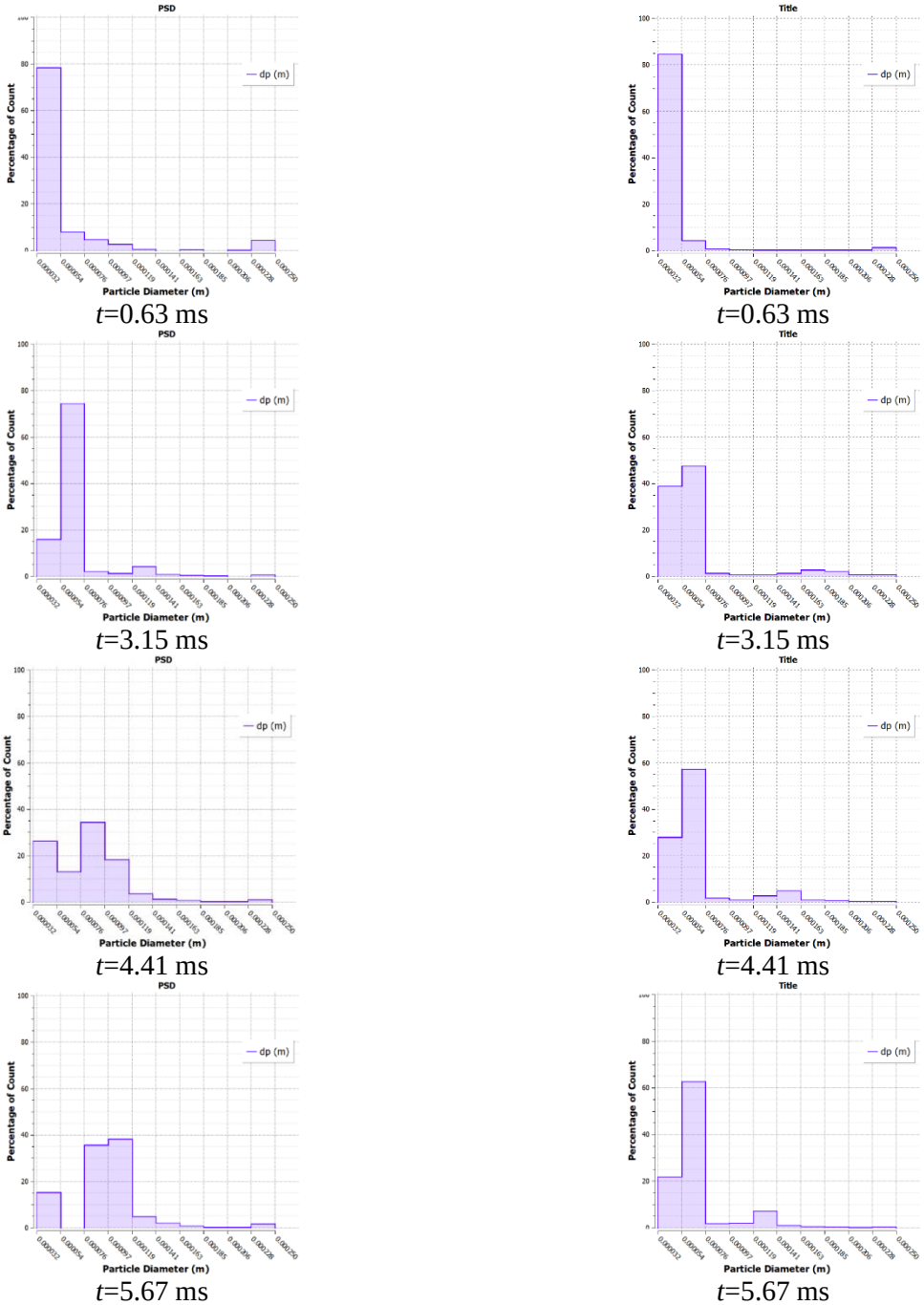

Figure 16 PSD of different injection type at different times after start of injection. Left: single type injection. Right: surface Type Injection.

6 Conclusion.

In this paper, particle size distribution in turbulent jet flow is investigated in 2D simulation. A configuration similar to a novel burner developed by Duisburg University [1] was employed for the current numerical simulation. The only difference is that, the current work focuses on a non-reacting flow (without considering the reaction) to examine the fluid flow field, heat transfer, and droplet size distribution. ANSYS-FLUENT V19.1 was used for meshing, simulation and postprocessing. In this work four different parameters were investigated (1) injection liquid velocity, (2) injection nozzle radius, (3) injected liquid type, and (4) injection

model. The impact of these parameters on flow field, temperature, and droplet size distribution can be summarized as follows:

- Increasing the injection liquid velocity from u_j=30 m/s to 91.34 m/s enhances the heat transfer and breakup where high injection speed, u_j =91.34 results in higher rate of heat transferred from the gas to the liquid by pulling the hot air (jet entrainment) to the core region. Higher injection speed results in faster heat transfer from the gas to the liquid; also, higher injection velocity would create smaller particles sizes (in ranges of $32\ \mu m\ to\ 126\ \mu m$) due to the breakup.
- Increasing the nozzle radius allows the spray to injected with higher mass flow rate, hence the rate of heat transfer is enhanced, which increases the liquid jet breakup on the other hand, the case with r = 0.75 mm (low Reynolds number) the droplets residence time increases and hence droplets have time to exchange the heat and breakup to produces smaller droplet with diameter $< 67\ \mu m$.
- Varying the physical and thermodynamics properties, the injected liquid (ethanol and n-heptane). It has been found that the gaseous flow field showed insignificant change. On the other hand, the rate of heat transfer between the gas and ethanol is higher than n-heptane. This is due to the high thermal conductivity and specific heat of ethanol compare with the n-heptane. The changes in PSD between the two liquids starts to be observed at t=5.67 ms after start of injection. The ethanol has a high particle temperature than n-heptane, hence, the breakup becomes more observed in the case of the ethanol case compared to n-heptane.
- Changing the type of injection model (single type injection / surface type injection) has no immediate effect on the particle size distribution. With time, the simulations with both modes diverge from each other. Whereas smaller droplets formed in the case of surface type injection compared to single injection, which shows more bigger particles. More calibration and evaluation for these models are needed in our future publications.

7 Data Availability

The data that support the findings of this study are available from the corresponding author upon reasonable request.

8 References

[1] F. Schneider, S. Suleiman, J. Menser, I. Wlokas, A. Kempf, H. Wiggers and C. Schulz, "SpraySyn—A standardized burner configuration for nanoparticle synthesis in spray flames," *scitation,* vol. 90, no. 8, 2019.

[2] N. El Sayed, H. Sumitomo and K. Masamichi, "Experimental and analytical investigation of liquid sheet breakup characteristics," *International Journal of Heat and Fluid Flow,* vol. 32, no. 1, pp. 95-106, 2011.

[3] F. Martins , A. Kronenburg and F. Beyrau, "PIV measurements under reacting and non-reacting conditions at the nozzle outlet of the SPP1980 SpraySyn burner," in *13th International Symposium on Particle Image Velocimetry,* Munich, Germany, 2019.

[4] F. Malte, B. Stodt, J. Kiefer and U. Fritsching, "Ethanol droplet formation, dynamics and combustion mode," *Experiments in Fluids,* vol. 10, pp. 60-125, 2019.

[5] M. Bieber, M. Al-Khatib, F. Fröde, H. Pitsch, M. A. Reddemann, H.-J. Schmid, R. Tischendorf and R. Kneer, "Influence of angled dispersion gas on coaxial atomization, spray and flame formation in the context of spray-flame synthesis of nanoparticles," *Experiments in Fluids,* vol. 10, pp. 62-98, 2021.

[6] X. Wang and H. Zhao, "Numerical simulation of the gasoline spray with an outward-opening piezoelectric injector: a comparative study of different breakup models," *SAE International,* vol. 01, 2018.

[7] R. Reitz and R. Diwakar, "Effect of drop breakup on fuel sprays," *SAE Technical,* vol. 95, pp. 218-227, 1986.

[8] R. Retiz, "Modeling atomization processes in high- pressure vaporizing sprays," *Atomisation and Spray Technology,* vol. 3, no. 4, pp. 309-337, 1987.

[9] G. Ingram Taylor, "The instability of liquid surfaces when accelerated in a direction perpendicular to their planes.," *Proceedings of the Royal Society A. Mathematical, Physical and Engineering Sciences,* vol. 201, no. 1065, 1950.

[10] R. D. Reitz and J. Beale, "Modeling spray atomization with the Kelvin-Helmholtz/ Rayleigh-Taylor hybrid model," *Atomization and Sprays,* vol. 9, no. 6, pp. 623-650, 1999.

[11] Amsden, P. O'Rourke and A. Anthony, "The TAB method for mumerical calculation of spray droplet breakup," *SAE Technical Paper,* 1987.

[12] A. Ann and M. Fergusson, ""Numerical simulation of a fuel nozzle's spray"," Ryerson University, Toronto, Ontario, Canada, 2011.

[13] M. Rosello, G. Maitrejean, D. Roux, P. Jay, B. Barbet and J. Xing, "Influence of the nozzle shape on the breakup behaviour of continuous ink jets," Researchgate, Grenoble, France, 2017.

[14] C. Sula, H. Grosshans and M. V. Papalexandris, "Assessment of droplet breakup models for spray flow simulations," *Springer Nature,* vol. 105, pp. 889-914, 2020.

[15] Y. Ren and X. Li, "Assessment and validation of liquid breakup models for high-pressure dense diesel sprays," *Front Energy,* vol. 10, pp. 164-175, 2016.

[16] S. Sapee, "Computational fluid dynamics study on droplet size of kerosene fuel," *Advanced Research in Fluid Mechanics and Thermal Sciences,* vol. 16, no. 1, pp. 1-14, 2015.

[17] C. Weise, M. Jan, K. Sebastian and A. Kempf, "Numerical investigation of the process steps in a spray flame reactor for nanoparticle synthesis," *Proceedings of the Combustion Institute,* vol. 35, no. 2, pp. 2259-2266, 2015.

[18] R. Fraser, P. Eisenklam, N. Domrowski and D. Hasson, "Drop formation from rapidly moving sheets," *AICHE,* pp. 672-680, 1962.